Biogeosciences Discuss., 11, 17339–17360, 2014
www.biogeosciences-discuss.net/11/17339/2014/
doi:10.5194/bgd-11-17339-2014

Biogeosciences
Discussions
Open Access

Radiative forcing bias of surface albedo modifications linked to simulated forest cover changes at northern latitudes

R. M. Bright[1], G. Myhre[2], R. Astrup[3], C. Antón-Fernández[3], and A. H. Strømman[1]

[1]Industrial Ecology Program, Energy and Process Engineering, Norwegian University of Science and Technology, Sem Sælands vei 7, E-1, 7491 Trondheim, Norway
[2]Center for Intenational Climate and Environmental Research – Oslo (CICERO), P.O. Box 1129, Blindern, 0318 Oslo, Norway
[3]Norwegian Forest and Landscape Institute, P.O. Box 115, 1431 Ås, Norway

Received: 24 October 2014 – Accepted: 15 November 2014 – Published: 12 December 2014

Correspondence to: R. M. Bright (ryan.m.bright@ntnu.no)

Published by Copernicus Publications on behalf of the European Geosciences Union.

Abstract

Simulated land use/land cover change (LULCC) radiative forcings (RF) from changes in surface albedo ($\Delta\alpha$) predicted by land surface schemes of six leading climate models were compared to those based on daily MODIS retrievals for three regions in Norway and for three winter–spring seasons. As expected, the magnitude and sign of the albedo biases varied considerably for forests; unexpectedly, however, biases of equal magnitude were evident in predictions at open area sites. The latter were mostly positive and exacerbated the strength of vegetation masking effects and hence the simulated LULCC $\Delta\alpha$ RF. RF bias was considerably small across models ($-0.08 \pm 0.04\,\mathrm{W\,m^{-2}}$; $21 \pm 11\,\%$); 4 of 6 models had normalized mean absolute errors less than 20 % (3-year regional mean). Identifying systematic sources of the albedo prediction biases proved challenging, although for some schemes clear sources were identified. Our study should provide some reassurance that model improvement efforts of recent years are leading to enhanced LULCC climate predictions.

1 Introduction

Albedo change radiative perturbations due to land use and land cover change (LULCC) have long been considered some of the strongest climate forcing mechanisms at global and regional scales (Cess, 1978; Otterman, 1977), yet results from recent historical LULCC modeling studies reveal an order or magnitude spread in the temperature response from albedo change forcings (Brovkin et al., 2006; Lawrence et al., 2012; Pongratz et al., 2010). This is likely because, in regions and months with snow cover, the interactions between vegetation and snow significantly complicate the relationship between the change in forest cover fraction and surface albedo (α_s) (de Noblet-Ducoudré et al., 2012). Outcomes of model inter-comparison studies (LUCID) employing identical LULCC prescriptions suggest that, apart from the way individual land surface models (LSMs) implement LULCC in their own land cover map (i.e.,

BGD
11, 17339–17360, 2014

differences in biogeography), model differences in the way α_s is parameterized could be a significant source of this spread (de Noblet-Ducoudré et al., 2012; Pitman et al., 2009). Recent attributional analysis by Boisier et al. (2012) suggests that the contribution from the latter is indeed comparable to the former and worthy of further investigation, particularly given the importance of albedo radiative feedbacks when ground or canopy surfaces are covered in snow (Crook and Forster, 2014; Hall and Qu, 2006).

Simulated α_s over snow-covered forests by climate models is often biased high (Essery, 2013; Loranty et al., 2014; Roesch, 2006). While most climate models distinguish between snow intercepted in forest canopies and snow on the ground, many differ in how they parameterize the fractions of ground and canopy that are covered with snow for given masses of lying and intercepted snow (Essery, 2013; Qu and Hall, 2007). This is likely because, rather than trying to simulate the complex processes of canopy snow interception and unloading as is done by many sophisticated, physically-based snow models (Essery et al., 2013, 2009) – many climate models must employ simplified parameterizations to reduce computational demands. In their assessment of α_s feedbacks simulated by 14 CMIP5 models, Qu and Hall (2014) find the largest intermodal spread in α_s occurring in northern latitude regions and suspect it to be behind the differences in the large range of local feedbacks. As with their previous inter-comparison analysis (Qu and Hall, 2007), Qu and Hall (2014) assert that parameterizations of snow masking in many CMIP5 models may still require improvement, suggesting further that winter observations over heavily vegetated surfaces such as the boreal forest should be used to constrain modeled α_s because of the vastly different parameterizations employed in the CMIP5 models for vegetation snow masking.

We hypothesize that parameterizations of snow masking by vegetation can be refined and improved in many climate models and that local calibration with empirical observation can enhance prediction accuracy. To this end, we evaluate α_s parameterization schemes of six prominent climate models in greater detail in order

Discussion Paper | Discussion Paper | Discussion Paper | Discussion Paper |

BGD

11, 17339–17360, 2014

On albedo bias in climate models

R. M. Bright et al.

to pinpoint major sources of bias and inter-model variability. Using a comprehensive empirical dataset of forest structure, meteorology, and daily MODIS α_s retrievals spanning three winter-spring seasons in three case regions of boreal Norway, we then estimate $\Delta\alpha_s$ radiative forcings connected to simulated forest cover changes (LULCC) and compare it to the MODIS-based forcings. We then develop a physically-based regression model and compare its performance to existing model schemes, concluding with a discussion surrounding the efforts required to improve albedo prediction accuracy in climate models.

2 Material and methods

We employed Version 006 (v006) MCD43A 1 day daily Albedo/BRDF product (Wang and Schaaf, 2013; Wang et al., 2012), taking the direct beam ("black-sky") α_s at local solar noon for the winter–spring seasons spanning 1 January 2007 through 9 May 2009. The v006 product uses multiple clear sky views available over a 16 day period to provide daily α_s values that represent the best BRDF possible with the day of interest emphasized. This includes as many overpasses that are available per day (while earlier versions of the algorithm, including the Direct Broadcast version, were limited to only 4 observations per day; Shuai, 2010), enabling it to better capture the daily albedo with an algorithm that more strongly emphasizes all contributions from the single day of interest (Wright et al., 2014).

Structural attributes like leaf area index (LAI), canopy height, and canopy cover fraction were derived from regional aerial LIght Detection and Ranging (LIDAR) campaigns undertaken in June of 2009 following Solberg et al. (2009). Daily meteorological observations of mean and maximum wind speed ($\mathrm{m\,s^{-1}}$), mean and maximum near-surface temperature (°C), snow depth (cm), and precipitation (mm) were taken from measuring stations in the municipalities of Drevsjø (675 m), Flisa (200 m), and Rena (250 m) located in eastern Norway in the county of Hedmark (Fig. S1 in the Supplement) (Norwegian Meteorological Institute, 2013). All three sub-regions

BGD
11, 17339–17360, 2014
On albedo bias in climate models
R. M. Bright et al.

lie in Köppen–Geiger climate zone "Dsc" (boreal) but experience variations in snow fall amount and frequency and the temporal extent of the snow cover season (additional meteorological information may be found in the Supplement and Fig. S2).

Local forest management plans were used to identify forest stands of pure (> 95 % volume, $m^3\,ha^{-1}$) evergreen needleleaf forest cover within a ~ 5 km radius and ~ 50 m altitude range of a weather monitoring station. Evergreen needleleaf species in the region included Scots Pine (*Pinus sylvestris* L.) and Norway Spruce (*Picea abies* (L.) H. Karst.). 12 open area sites within the same 5 km proximity to a weather station were selected in order to simulate forcings associated with regional LULCC (forest to open). In total, 250 forested MODIS pixels (approximately 5300 ha) and 12 open area pixels (8 cropland, 4 wetland/peatland) were included in the sample (Fig. S1).

2.1 Albedo parameterizations in climate models

The particular land surface models chosen for analysis (Table 1) were selected because they are widely employed in climate/earth system models and because their α_s schemes are diverse with respect to the parameterization of ground masking by vegetation, which can be classified according to three prevailing methods introduced in Qu and Hall (2007) (and later described in Essery, 2013). Briefly, the first method estimates radiative transfer between the vegetation canopy and the ground surface; the second method combines the vegetation and ground albedos with weights determined by vegetation cover; and the third method combines the snow-free and snow albedo with weights determined by snow cover. Varying degrees of model complexity stem from the way snow albedo metamorphosis effects are parameterized and the way vegetation structure is utilized (Sect. S3 in the Supplement).

2.2 Regression modeling

Non-linear multiple regressions are performed using the forest structure and meteorological observations as predictor variables. The functional form of the models

BGD
11, 17339–17360, 2014

are adapted from several important physically-based parameterizations found in many current albedo schemes. Equation (1) is the best performing model:

$$\alpha_s = k_1 + k_2(1 - e^{-\mathrm{LAI}}) + k_3 \tanh(d/k_4)\left(e^{-k_5(\mathrm{LAI})} + \left[1 - \frac{1}{1 + e^{-k_6 T^{\mathrm{Max}}}}\right]\right) \tag{1}$$

where LAI, d, and T^{Max} are leaf area index, snow depth, and maximum daily (24 h) temperature, respectively. k_1 is the ground albedo (directional hemispherical) without the forest canopy scaled by a canopy radiative fraction term $(1 - e^{-\mathrm{LAI}})$ and the parameter k_2, with k_2 representing the maximum albedo difference at the highest observed LAI values. See the Supplement (Sect. S4) for a detailed overview and description of the regression model and its theoretical underpinnings, its parameters (Table S6), and its performance statistics (Table S6).

2.3 Radiative forcing

Top-of-atmosphere (TOA) radiative forcing simulations for the conversion of evergreen needleleaf forest to open land ($\Delta\alpha_s$, Open – Forest) is computed using a 3-D four spectral band, eight-stream radiative transfer model (Myhre et al., 2007) based on the discrete ordinate method (Stamnes et al., 1988). The model is run with a 3 h time step with a horizontal resolution of $1^\circ \times 1^\circ$ and a vertical resolution of 40 layers. Meteorological data from the ECMWF is used in the radiative transfer simulations and several atmospheric aerosol types are included in the model (Myhre et al., 2007). Regional RF from LULCC is estimated by changing the monthly mean α_s of the entire grid cell and normalizing to the share of existing cropland contained within each grid cell.

3 Results

3.1 Albedo

When looking at regional averages in predicted α_s presented in Fig. 1, no single model apart from the regression model ("REG") performed consistently well across all months at both Forest and Open sites and for both spectral bands. Starting with the NIR band (Fig. 1, left column), JSBACH showed clear positive biases at both Open and Forest sites for most months. Positive biases in GISS II were more prevalent for Forest although positive biases were also found at Open sites for months with partial snow cover (November, April, May). Large positive biases for the JULES 2-stream ("JUL-2") scheme were limited to Forest and to winter months of January, February, and March. With the exception of February, slight negative biases by JUL-2 at the Open sites were found in all months except February; this was true also for the JULES All-band scheme ("JUL-AB") with the exception of March. The largest difference between the two JULES schemes occurred for Forest, where JUL-AB consistently underpredicted α_s in all months except May. Large negative biases in Forest by CLASS were found in November and January with smaller negative biases in February.

Moving on to the VIS band (Fig. 1, right column), most schemes overpredicted α_s during winter months (January–March) at the Open sites. The largest spread (i.e., standard deviation, SD) at the Open sites occurred during November (SD = 0.08), where the largest negative bias was found for CLM4 and positive bias for JSBACH. Like in the NIR band, results varied more at the Forest sites where biases across months were more evenly distributed around zero ($r = 1$). Again, here we found positive biases by JUL-2 yet negative biases by JUL-AB during January–April Positive biases by JSBACH were mostly confined to November, January, and February at both Open and Forest sites. Unlike the NIR band in which positive biases at Open sites by GISS II were limited to November, April, and May – for the VIS band positive biases occurred in all months; however, the positive biases in Forests seen for the NIR band during

November, February, and April were reduced. Like the NIR band, large negative biases were found for CLASS for November, January, and February.

In general, Fig. 1 shows that the inter-model spread was smaller for the VIS band predictions relative to NIR, and at Open sits relative to Forest sites. Figure 1 also indicates that the inter-model spread in α_s predictions for both bands and land cover types was larger during November–February and smaller during March–May. With the exception of JUL-2 in the NIR band, all models overpredicted November–May mean $\Delta\alpha_s$ (Fig. 1e and f, "Open – Forest") in both spectral bands. Models with negative α_s biases at Forest sites and positive α_s biases at Open sites – such as CLASS and JUL-AB – led to some of the largest positive $\Delta\alpha_s$ biases. For some schemes like GISS II and JSBACH, positive α_s biases at both Open and Forest sites offset each other resulting in low $\Delta\alpha_s$ biases, particularly in the NIR band. Only for the NIR band (Fig. 1e) did any model underpredict $\Delta\alpha_s$. Here, JUL-2 under- and overpredicted α_s at Forest and Open sites, respectively.

Monthly α_s biases were often reduced when weighted by the relative share of monthly insolation during November–May, as seen in Fig. 1 particularly for the JSBACH and CLASS schemes, which suggests that a large share of the bias occurred during winter months.

3.2 Radiative forcing

November–May mean (2007–2009) TOA RF from simulated LULCC ($\Delta\alpha$, Open – Forest) are presented in Fig. 2a for each of the three case study regions. In Rena and Drevsjø, all models overpredicted $\Delta\alpha_s$ and thus simulated LULCC RF. No clear patterns emerged regarding relationships between RF error, model, and study region; RF errors by REG, CLM4, and CLASS were larger in Rena (green bars) relative to Drevsjø (red bars) – while RF errors were larger for the JULES models, JSBACH, and GISS II for Drevsjø relative to Rena. One would expect a larger spread in the modeled RF for Drevsjø given the larger inherent variability in vegetation structure in the forest sample (Table S1) and given the fundamental differences in the way each albedo scheme handles vegetation structure (Sec. S3), yet we found the largest inter-model spread occurring in Rena (RF SD = 0.075), where the normalized mean errors (NME) ranged from 6–58 % for JSBACH and CLASS, respectively (Fig. 2b, green right-hand y axis). For Drevsjø, the inter-model spread was smaller (RF SD = 0.067), with RF NME ranging from 14–54 % for CLM4 and JUL-AB respectively. One possible explanation is that Rena experienced more frequent precipitation events, more fluctuating maximum daily temperature (above and below freezing), and a snowpack that tended to melt more rapidly in early spring than in Drevsjø (Fig. S2) – all of which complicated the prediction of ground and forest canopy α_s in the presence of snow.

The inter-model spread was lowest in Flisa (RF SD = 0.05), with RF NME ranging from 2 % for the Regression model and 22 % for CLASS, respectively. In Flisa, JSBACH and JUL-AB underestimated the strength of the vegetation masking effect ($\Delta\alpha_s$ bias) and thus the simulated LULCC RF. Together with CLASS, these two schemes also led to some of the largest RF spreads across sub-regions by any single model, where RF NME for JUL-AB ranged 10–54 % for Flisa and Drevsjø, respectively; for CLASS 22–58 % for Flisa and Rena, respectively; and for JSBACH from 6–32 % for Flisa and Drevsjø, respectively.

For JSBACH, the result of having both positive and negative $\Delta\alpha_s$ biases is a regional mean RF (Fig. 2a, grey bar) that most closely resembled the MODIS based RF; with MAE (or NME) as a metric, however, JSBACH only ranked 3rd of 7 (Fig. 2b, top). Although not ranked 1st in all sub-regions, REG led to the most accurate regional mean RF prediction (MAE/NME, Fig. 2b, grey).

It is worth reiterating that some schemes such as that of GISS II severely overpredicted α_s at both Open and Forest sites (Table 3) which was not reflected in $\Delta\alpha_s$ or $\Delta\alpha_s$ RF, thereby giving the impression that the scheme ranked relatively high in accuracy.

BGD
11, 17339–17360, 2014

4 Discussion

We hypothesized that climate model parameterizations of vegetation masking effects on surface albedo in boreal winter and spring could be further refined and improved in land surface models to increase prediction accuracy, although it is evident from our analysis that – for evergreen needleleaf forests – most of the existing schemes already do a reasonably good job at predicting α_s in the presence of snow, leaving little room for improvement. Given the multitude of vegetation structural, meteorological, and other site-specific physical factors involved in shaping the total α_s of the forest canopy and underlying surface, normalized mean absolute prediction error (NME) of < 20 % in our $\Delta\alpha_s$ RF simulations is considered a remarkably high accuracy for climate models that must depend on reduced complexity schemes (relative to 3-D radiative transfer models or sophisticated snow-ice physics models).

A surprising finding of our study is that parameterizations of Open area α_s – which is governed mostly by the albedo of snow from January through early April – contributed as much to $\Delta\alpha_s$ prediction error as that of Forests (Fig. 1). The bias was mostly positive although there is some evidence that MODIS may underestimate the albedo of cold dry snow (Jin et al., 2002; Stroeve et al., 2005; Wang and Zender, 2010) – particularly in VIS bands (Wang and Zender, 2010). Jin et al. (2002), for example, assert that there may be up to a 10 % negative bias in the MODIS pure dry snow albedo (Jin et al., 2002), which could partially explain why most models in our study tended to overestimate α_s during the coldest months of January and February (Fig. 1). Factoring in any potential negative MODIS snow α_s bias would reduce some of the positive open area biases (Fig. 1; Supplement) but not all of it, particularly for CLASS and JSBACH, whose positive open area α_s biases were particularly large during months with snow cover. Snow α_s was reset to a maximum after a fresh snowfall event (Tables S3 and S4); however, MODIS albedo retrievals were far below the prescribed maximum snow albedo values of these two schemes after fresh snowfall events (Figs. S24–S26 for JSBACH and Figs. S30–S32 for CLASS), particularly for the VIS band.

BGD
11, 17339–17360, 2014

The two schemes with regional mean RF NMEs (Fig. 2b) above 20 % were the CLASS and JUL-AB schemes. For CLASS, RF NME > 20 % was realized for all three sub-regions. The $\Delta\alpha_s$ RF bias of CLASS was due to overpredictions at open area sites and underpredictions at forested sites. The latter is due to the parameterization of canopy transmittance that is based on an extinction coefficient that incorporates a correction factor of 0.3 and 0.4 for NIR and VIS bands, respectively (Eqs. S10 and S11 in the Supplement). Lowering these to 0.25 and 0.3 for NIR and VIS bands, respectively, serves to reduce the negative biases in forests, particularly at high solar zenith angles (November–February). As aforementioned, at the open sites the VIS albedo constant of 0.95 for fresh snow was too high; the maximum observed VIS albedo after a fresh snowfall event was 0.88 (all study regions), and adjusting to 0.90 would alleviate some of this bias (disregarding potential MODIS biases).

Although JUL-AB (formerly MOSES v. 2.2) ranked 6th/7 overall when considering only the regional mean RF MAE and NME (Table 4), in two of the three study regions (Flisa and Rena) it performed quite well, with RF NMEs of < 11 % and < 16 % for Flisa and Rena, respectively. The large RF NME for Drevsjø was a result of a severe negative bias in the predicted α_s of forests (Fig. S11), which resulted in large positive $\Delta\alpha_s$ biases (Table S3). The explanation is due to the use of vegetation-specific snow albedo parameters that were too low for forests in this region – forests that were characterized as having the lowest median tree heights, LAIs, and canopy cover fractions out of the three forested sub-regions (Table S1).

Of the existing land model schemes included in this study, JUL-2 performed best in the LULCC RF simulations (Fig. 2), although we note that it underestimated the strength of the vegetation masking effect ($\Delta\alpha_s$) in the NIR band while overestimating it in the VIS band (Fig. 1) (consistent across all three study regions, Table S3) which may have had offsetting effects in the RF simulations. A closer inspection of the daily α_s time series (Sect. S5.2) hints that forest albedo (Figs. S15–S17) may be too sensitive to snow depth (Fig. S2) – an important variable in the parameterization of snow cover fraction (Eq. S2). For example, α_s predictions were biased positive at snow depths

Discussion Paper | Discussion Paper | Discussion Paper | Discussion Paper |

BGD

11, 17339–17360, 2014

On albedo bias in climate models

R. M. Bright et al.

above 0.6 m (typical in Rena and Drevsjø during the winter-spring of 2008 and 2009) while biased negative at Flisa during 2007 and 2008 for which snow depths never exceeded 0.4 m. This same sensitivity of forest α_s on snow depth was also found for the GISS II scheme – another Type 3 scheme – resulting in positive α_s biases in forests. This sensitivity to snow depth was not evident for JUL-AB – the third Type 3 scheme. This is because, unlike GISS II and JUL-2, snow albedo is vegetation-dependent and constrained by satellite observation (MODIS).

In agreement with findings in Essery (2013), we generally find that no single type of scheme (as described in Sect. 2.1 and in Qu and Hall, 2007) stood out as performing better or worse relative to the others. In their latest CMIP5 simulations, Qu and Hall (2014) assert that type 2 schemes – or those which parameterize albedo as a function of vegetation cover rather than snow cover – generally tended to overestimate the strength of the snow albedo masking effect ($\Delta\alpha_s$) due to negative biases in forest α_s predictions. For JSBACH – a Type 2 scheme – we did not detect this bias; rather, we found positive biases in Forest in both bands, particularly during the snow season which is consistent with findings of Brovkin et al. (2013) and Hagemann et al. (2013). NIR albedo predictions in Flisa and Rena during snow-free periods were also biased high (figures in Sect. S5.4) resulting in underestimations of NIR $\Delta\alpha_s$, which we attributed to a snow-free vegetation albedo constant that was too high (Table S4). The positive RF bias seen at Drevsjø (Fig. 2) stemmed from negative biases in the springtime (March–May) VIS α_s in forests (Fig. S29). This may be attributed to the default use of 1 as the stem area index (SAI) used in the masking parameterization (Reick et al., 2012); observational evidence suggests this may be too high in boreal regions in spring (Lawrence and Chase, 2007).

While the simulated $\Delta\alpha_s$ RF by GISS II appeared relatively robust (Fig. 2), α_s predictions in Forest and Open were strongly positively biased in both spectral bands. In forests, this could be attributed to two main factors: (i) a dependence on snow-free albedo constants that were too high, particularly when applied at the denser (i.e., high CC%, Table S1) sites of Flisa and Rena, (ii) a strong dependency on snow depth and/or

BGD
11, 17339–17360, 2014

lack of explicit representation of forest structure in the masking expression which led to overpredictions in Rena and Drevsjø (Figs. S40 and S41) – regions that experienced snow depths greater than 60 cm for much of the winter and early spring in 2008 and 2009 (March–late April). NIR biases at the open sites (Figs. S36–S38) were attributed to the use of snow-free vegetation constants that were too high (Table S5).

Sources of RF biases in CLM4 were harder to discern, as the sign of the predicted $\Delta\alpha_s$ bias was not consistent across study sites and months. $\Delta\alpha_s$ bias was negative and mostly limited to March and April at Flisa and Rena (Table S3). $\Delta\alpha_s$ bias was positive at Drevsjø and occurred mostly in April and May due to overpredictions in both NIR and VIS α_s in Forest and underpredictions in both NIR and VIS α_s at Open sites (Figs. S18–S23).

Not surprisingly, the purely empirical α_s model presented here (Eq. 1) calibrated with local forest structure and meteorological observations performed best on average throughout the region (i.e., Fig. 2; MAE, NME, and Rank). However, to our surprise, it did not rank first in all study regions; it ranked 5th in Rena which was the region having the fewest forest structure, meteorological, and MODIS albedo retrievals. This highlights the high performance dependencies of purely empirically-based models to the underlying datasets to which they are calibrated. Although it is tempting to recommend its application over existing modeling schemes in boreal regions, rigorous evaluation efforts would be needed to assess the degree of transportability and reliability when applied in other regions having different forest structures and climate regimes (Bright et al., 2014).

5 Conclusions

Simulated seasonal LULCC radiative forcings (RF) from changes in land surface albedo ($\Delta\alpha_s$) predicted by six of the world's leading climate models were evaluated using observed meteorology and forest structure for a case region in Norway and by comparing to MODIS daily albedo retrievals. Compared to RF simulations based

BGD
11, 17339–17360, 2014

on MODIS albedo, all six models plus an additional empirical model developed here overestimated the magnitude of the simulated regional mean RF (Fig. 2) by overestimating $\Delta\alpha_s$ (Fig. 1), although results varied between three sub-regions within the broader case study region. For instance, in a sub-region characterized as having the highest forest productivity and lowest seasonal snow cover of the three (Flisa), two of the models underestimated $\Delta\alpha_s$ RF (JSBACH and JULES All-band).

Efforts to uncover sources of systematic albedo biases proved challenging as no clear discernible patterns could be detected across study regions or between the different types of schemes (Sect. 2.1), although some systematic sources of bias in forest α_s were identified for the CLASS, JULES All-band, JSBACH, and GISS II schemes. Severe negative albedo bias in winter months by CLASS – evident across all three study regions – was attributed to the parameterization of canopy transmittance. For GISS II, persistent positive α_s biases were linked to snow-free vegetation albedos (both VIS and NIR bands) that were too high and to a snow cover masking parameterization that did not explicitly account for differences in forest structure. Biases in forests in the JULES All-band scheme can be easily alleviated by adjusting (in our case increasing) the vegetation-dependent snow albedo values for "Evergreen Needleleaf" forest, which, in our study, were based on MODIS latitude band averages (Gao et al., 2005). Similarly for JSBACH, forest biases can be easily reduced by lowering the snow-free vegetation albedo value in the NIR band.

Nevertheless, given the complexities involved in parameterzing the albedo of forests in boreal winter and spring (in the presence of snow), given the diversity of climate regimes and forest structure types that models must be designed to accommodate, and given the reduced complexity requirements of albedo parameterizations by global climate models – our study should give some reassurance to climate modelers that recent efforts to improved parameterizations of vegetation masking effects are leading to more accurate predictions of surface albedo and hence climate change predictions linked to LULCC.

The Supplement related to this article is available online at doi:10.5194/bgd-11-17339-2014-supplement.

Acknowledgements. We thank Zhuosen Wang and Crystal Schaaf for the preparation of the MODIS 1 day albedo dataset, without which this study would not have been possible. All empirical datasets – including forest structure, meteorology, and MODIS albedo – can be made available upon request. This work was performed under the project "Decision Support Models for Increased Harvest and Climate-motivated Forest Policies" funded by the Norwegian Research Council, grant number: 210464.

References

Best, M.: JULES Technical Documentation, Met Office, Joint Centre for Hydro-Meteorological Research, Wallingford, UK, 2009.

Boisier, J. P., de Noblet-Ducoudré, N., Pitman, A. J., Cruz, F. T., Delire, C., van den Hurk, B. J. J. M., van der Molen, M. K., Müller, C., and Voldoire, A.: Attributing the impacts of land-cover changes in temperate regions on surface temperature and heat fluxes to specific causes: results from the first LUCID set of simulations, J. Geophys. Res., 117, D12116, doi:10.1029/2011JD017106, 2012.

Bright, R. M., Antón-Fernández, C., Astrup, R., and Strømman, A. H.: Empirical models of albedo transitions in managed boreal forests: analysis of performance and transportability, Can. J. Forest Res., doi:10.1139/cjfr-2014-0132, online first, 2014.

Brovkin, V., Claussen, M., Driesschaert, E., Fichefet, T., Kicklighter, D., Loutre, M. F., Matthews, H. D., Ramankutty, N., Schaeffer, M., and Sokolov, A.: Biogeophysical effects of historical land cover changes simulated by six Earth system models of intermediate complexity, Clim. Dynam., 26, 587–600, 2006.

Brovkin, V., Boysen, L., Raddatz, T., Gayler, V., Loew, A., and Claussen, M.: Evaluation of vegetation cover and land-surface albedo in MPI-ESM CMIP5 simulations, Journal of Advances in Modeling Earth Systems (JAMES), 5, 48–57, 2013.

Cess, R. D.: Biosphere–albedo feedback and climate modeling, J. Atmos. Sci., 35, 1765–1768, 1978.

BGD

11, 17339–17360, 2014

On albedo bias in climate models

R. M. Bright et al.

Crook, J. A. and Forster, P. M.: Comparison of surface albedo feedback in climate models and observations, Geophys. Res. Lett., 41, 1717–1723, doi:10.1002/2014GL05928, 2014.
de Noblet-Ducoudré, N., Boisier, J.-P., Pitman, A., Bonan, G. B., Brovkin, V., Cruz, F., Delire, C., Gayler, V., van den Hurk, B. J. J. M., Lawrence, P. J., van der Molen, M. K., Müller, C., Reick, C. H., Strengers, B. J., and Voldoire, A.: Determining robust impacts of land-use-induced land cover changes on surface climate over North America and Eurasia: results from the first set of LUCID experiments, J. Climate, 25, 3261–3281, 2012.
Dickinson, R. E.: Land surface processes and climate-surface albedos and energy balance, Adv. Geophys., 25, 305–353, 1983.
Essery, R.: Large-scale simulations of snow albedo masking by forests, Geophys. Res. Lett., 40, 5521–5525, 2013.
Essery, R., Best, M., and Cox, P.: MOSES 2.2 Technical documentation, Hadley Centre Technical Note 30, UK Met Office Hadley Centre, Exeter, UK, 1–31, 2001.
Essery, R., Rutter, N., Pomeroy, J. W., Baxter, R., Stähli, M., Gustafsson, D., Barr, A., Bartlett, P., and Elder, K.: SnowMIP2: An evaluation of forest snow process simulations, B. Am. Meteorol. Soc., 90, 1120–1135, doi:10.1175/2009BAMS2629.1, 2009
Essery, R., Morin, S., Lejeune, Y., and Ménard, C. B.: A comparison of 1701 snow models using observations from an alpine site, Adv. Water Resour., 55, 131–148, 2013.
Flanner, M. G. and Zender, C. S.: Linking snowpack microphysics and albedo evolution, J. Geophys. Res., 111, D12208, doi:10.1029/2005JD006834, 2006.
Gao, F., Schaaf, C. B., Strahler, A., H., Roesch, A., Lucht, W., and Dickinson, R. E.: MODIS bidirectional reflectance distribution function and albedo Climate Modeling Grid products and the variablility of albedo for major global vegetation types, J. Geophys. Res., 110, 1–13, 2005.
Hagemann, S., Loew, A., and Andersson, A.: Combined evaluation of MPI-ESM land surface water and energy fluxes, JAMES, 5, 259–286, 2013.
Hall, A. and Qu, X.: Using the current seasonal cycle to constrain snow albedo feedback in future climate change, Geophys. Res. Lett., 33, L03502, doi:10.1029/2005GL025127, 2006.
Hansen, J., Russell, G., Rind, D., Stone, P., Lacis, A., Lebedeef, S., Ruedy, R., and Travis, L.: Efficient three-dimensional global models for climate studies: models I and II, Mon. Weather Rev., 111, 609–662, 1983.

BGD
11, 17339–17360, 2014

On albedo bias in climate models

R. M. Bright et al.

Jin, Y., Schaaf, C. B., Gao, F., Li, X., Strahler, A. H., Zeng, X., and Dickinson, R. E.: How does snow impact the albedo of vegetated land surfaces as analyzed with MODIS data?, Geophys. Res. Lett., 29, 12-11–12-14, 2002.

Lawrence, P. J. and Chase, T. N.: Representing a new MODIS consistent land surface in the Community Land Model (CLM 3.0), J. Geophys. Res., 112, G01023, doi:10.1029/2006JG000168, 2007.

Lawrence, P. J., Feddema, J. J., Bonan, G. B., Meehl, G. A., O'Neill, B. C., Oleson, K. W., Levis, S., Lawrence, D. M., Kluzek, E., Lindsay, K., and Thornton, P. E.: Simulating the biogeochemical and biogeophysical impacts of transient land cover change and wood harvest in the Community Climate System Model (CCSM4) from 1850 to 2100, J. Climate, 25, 3071–3095, 2012.

Loranty, M. M., Berner, L. T., Goetz, S. J., Jin, Y., and Randerson, J. T.: Vegetation controls on northern high latitude snow-albedo feedback: observations and CMIP5 model simulations, Glob. Change Biol., 20, 594–606, 2014.

Marshall, S. E.: A physical parameterization of snow albedo for use in climate models. NCAR Cooperative Thesis 123, National Center for Atmospheric Research (NCAR), Boulder, Colorado, USA, 1989.

Matthews, E.: Prescription of Land-surface boundary conditions in GISS GCM II: a simple method based on high-resolution vegetation data bases, NASA Technical Memorandum 86096, NASA Goddard Institute for Space Studies, New York, NY, USA, 21 pp., 1984.

Myhre, G., Bellouin, N., Berglen, T. F., Berntsen, T. K., Boucher, O., Grini, A., Isaksen, I. S. A., Johnsrud, M., Mishchenko, M. I., Stordal, F., and Tanré, D.: Comparison of the radiative properties and direct radiative effect of aerosols from a global aerosol model and remote sensing data over ocean, Tellus B, 59, 115–129, doi:10.1111/j.1600-0889.2006.00226.x, 2007.

Norwegian Meteorological Institute: eKlima – Daily Historical Meteorology, Norwegian Meteorological Institute, available at: http://sharki.oslo.dnmi.no/portal/page?_pageid=73,39035,73_39049&_dad=portal&_schema=PORTAL (last access: 15 September 2013), 2013.

Oleson, K., Lawrence, D. M., Bonan, G. B., Flanner, M. G., Kluzek, E., Lawrence, P. J., Levis, S., Swenson, S. C., Thornton, P. E., Dai, A., Decker, M., Dickinson, R. E., Feddema, J. J., Heald, C. L., Hoffman, F., Lamarque, J. F., Mahowald, N., Niu, G.-Y., Qian, T., Randerson, J., Running, S. W., Sakaguchi, A. S., Stökli, R., Wang, A., Yang, Z.-L., Zeng, X., and Zeng, X.:

Technical Description of Version 4.0 of the Community Land Model (CLM), National Center for Atmospheric Research, Climate and Global Dynamics Division, Boulder, CO, USA, 266 pp., 2010.
Otterman, J.: Anthropogenic impact on the albedo of the earth, Climatic Change, 1, 137–155, 1977.
Otto, J., Raddatz, T., and Claussen, M.: Strength of forest-albedo feedback in mid-Holocene climate simulations, Clim. Past, 7, 1027–1039, doi:10.5194/cp-7-1027-2011, 2011.
Pitman, A. J., de Noblet-Ducoudré, N., Cruz, F. T., Davin, E. L., Bonan, G. B., Brovkin, V., Claussen, M., Delire, C., Ganzeveld, L., Gayler, V., van den Hurk, B. J. J. M., Lawrence, P. J., van der Molen, M. K., Müller, C., Reick, C. H., Seneviratne, S. I., Strengers, B. J., and Voldoire, A.: Uncertainties in climate responses to past land cover change: first results from the LUCID intercomparison study, Geophys. Res. Lett., 36, L14814, doi:10.1029/2009GL039076, 2009.
Pongratz, J., Reick, C. H., Raddatz, T., and Claussen, M.: Biogeophysical versus biogeochemical climate response to historical anthropogenic land cover change, Geophys. Res. Lett., 37, L08702, doi:10.1029/2010GL043010, 2010.
Qu, X. and Hall, A.: What controls the strength of snow–albedo feedback?, J. Climate, 20, 3971–3981, 2007.
Qu, X. and Hall, A.: On the persistent spread in snow-albedo feedback, Clim. Dynam., 42, 69–81, 2014.
Reick, C. H., Gayler, V., Raddatz, T., and Schnur, R.: JSBACH – the New Land Component of ECHAM, Max Planck Insitute for Meteorology, Hamburg, Germany, 1–167, 2012.
Roesch, A.: Evaluation of surface albedo and snow cover in AR4 coupled climate models, J. Geophys. Res.-Atmos., 111, D15111, doi:10.1029/2005JD006473, 2006.
Sellers, P. J.: Canopy reflectance, photosynthesis, and transpiration, Int. J. Remote Sens., 6, 1335–1372, 1985.
Shuai, Y.: Tracking Daily Land Surface Albedo and Reflectance Anisotropy with MODerate-Resolution Imaging Spectroradiometer (MODIS), Ph.D. thesis, Geography and Environment, Boston University, Boston, 2010.
Solberg, S., Brunner, A., Hanssen, K. H., Lange, H., Næsset, E., Rautiainen, M., and Stenberg, P.: Mapping LAI in a Norway spruce forest using airborne laser scanning, Remote Sens. Environ., 113, 2317–2327, 2009.

BGD
11, 17339–17360, 2014

On albedo bias in climate models

R. M. Bright et al.

Stamnes, K., Tsay, S. C., Wiscombe, W., and Jayaweera, K.: Numerically stable algorithm for discrete-ordinate-method radiative transfer in multiple scattering and emitting layered media, Appl. Optics, 27, 2502–2509, 1988.
Stroeve, J., Box, J. E., Gao, F., Liang, S., Nolin, A., and Schaaf, C.: Accuracy assessment of the MODIS 16-day albedo product for snow: comparisons with Greenland in situ measurements, Remote Sens. Environ., 94, 46–60, 2005.
Verseghy, D. L.: CLASS – the Canadian Land Surface Scheme (Version 3.4) – Technical Documentation (Version 1.1), Environment Canada, Quebec, Canada, 1–183, 2009.
Verseghy, D. L., McFarlane, N. A., and Lazare, M.: CLASS – a Canadian land surface scheme for GCMs. II. Vegetation model and coupled runs, Int. J. Climatol., 13, 347–370, 1993.
Wang, X. and Zender, C. S.: MODIS snow albedo bias at high solar zenith angles relative to theory and to in situ observations in Greenland, Remote Sens. Environ., 114, 563–575, 2010.
Wang, Z. and Schaaf, C.: MCD43 1-day and 16-day Daily Albedo/BRDF Dataset, University of Massachusetts, Boston and Boston University, 23 March 2013, Boston, 2013.
Wang, Z., Schaaf, C. B., Chopping, M. J., Strahler, A. H., Wang, J., Román, M. O., Rocha, A. V., Woodcock, C. E., and Shuai, Y.: Evaluation of Moderate-resolution Imaging Spectroradiometer (MODIS) snow albedo product (MCD43A) over tundra, Remote Sens. Environ., 117, 264–280, 2012.
Wiscombe, W. J. and Warren, S. G.: A model for the spectral albedo of snow. I. Pure Snow, J. Atmos. Sci., 37, 2712–2733, 1980.
Wright, P., Bergin, M., Dibb, J., Lefer, B., Domine, F., Carman, T., Carmagnola, C., Dumont, M., Courville, Z., Schaaf, C., and Wang, Z.: Comparing MODIS daily snow albedo to spectral albedo field measurements in Central Greenland, Remote Sens. Environ., 140, 118–129, 2014.

Table 1. Land models included in the study.

Land model (α_s scheme)	Climate model	Snow albedo	Vegetation masking effect[b]	Forest structure	Technical documentation	Other supporting references
CLASS	CGCM4; CanCM4	prognostic procedure	type 2	yes	Verseghy (2009)	Verseghy et al. (1993)
CLM4.0	NCAR CCSM4; NCAR CESM; Nor-ESM	prognostic procedure	type 1	yes	Oleson et al. (2010)	Dickinson (1983), Flanner and Zender (2006), Sellers (1985)
GISS II	GISS GCM II; GISS GCM ModelE	prognostic procedure	type 3	no	Hansen et al. (1983)	Matthews (1984)
JULES[a] (2-stream)	UKMO HadGEM2	prognostic procedure	type 3	yes	Best (2009)	Marshall (1989), Sellers (1985), Wiscombe and Warren (1980)
JULES[a] (all-band)	UKMO HadCM3	diagnostic procedure	type 3	yes	Best (2009)	Essery et al. (2001)
JSBACH	MPI-ESM	diagnostic procedure	type 2	yes	Reick et al. (2012)	Otto et al. (2011)

[a] Formerly MOSES.
[b] Classification based on Qu and Hall (2007).

BGD
11, 17339–17360, 2014
On albedo bias in climate models
R. M. Bright et al.

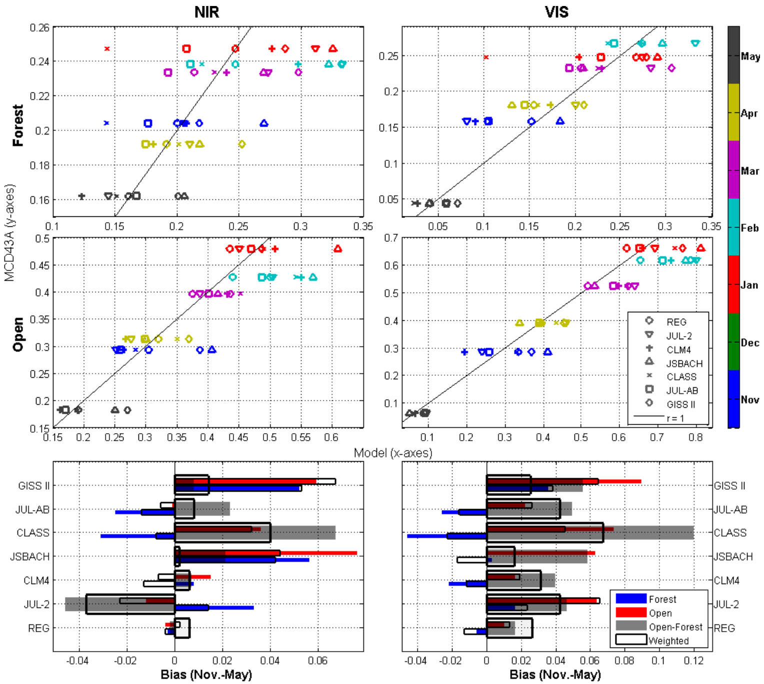

Figure 1. (a–d) Correlations between the observed (MCD43A, *y* axes) and modeled (*x* axes) direct-beam albedo (monthly means, 2007–2009) in evergreen needleleaf forests **(a, b)** and adjacent open areas **(c, d)** for both near-infrared (left column, "NIR") and visible bands (right column, "VIS") averaged across all three study regions; **(e)** NIR and **(f)** VIS November–May mean bias (regional and monthly means, 2007–2009) and insolation-weighted mean bias. High solar zenith angles inhibited the number of sufficient MODIS retrievals in December, thus December mean biases were excluded from the November–May mean; MB = $\frac{1}{N}\sum_{i=1}^{N}(\alpha_{\text{Model}} - \alpha_{\text{Obs.}})$.

BGD
11, 17339–17360, 2014

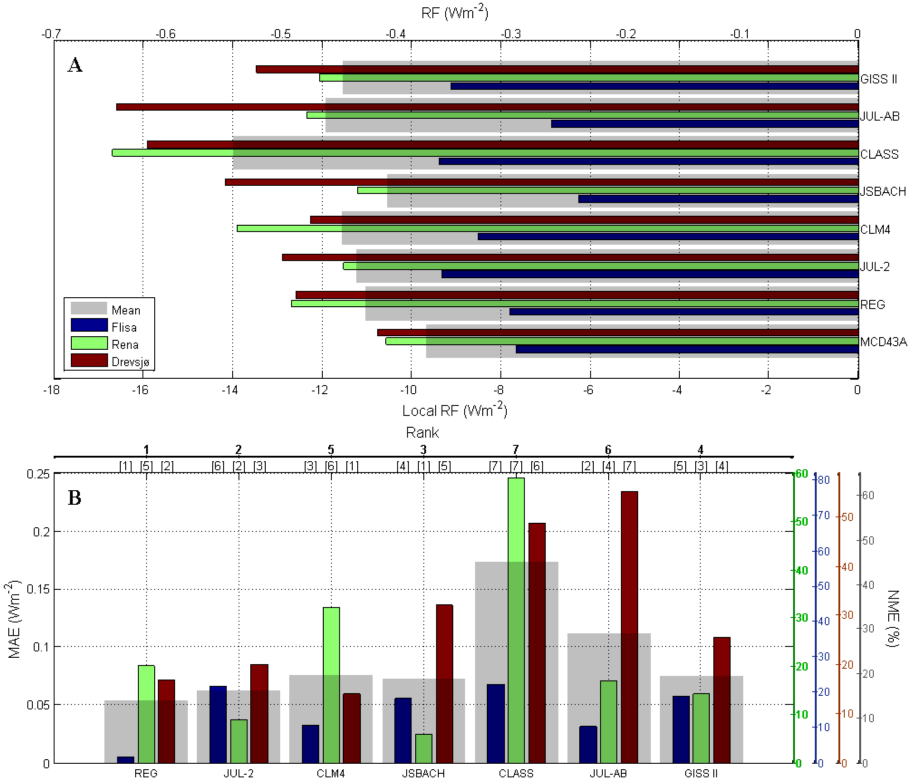

Figure 2. (a) Radiative forcing (RF) from simulated vs. observed (MCD43A) albedo changes (Open–Forest), 2007–2009 November–May mean (excluding December). The lower x axis shows the difference between Open and Forest, whereas the upper x axis show RF values weighted by the cropland fraction (same for all regions); **(b)** mean absolute error (MAE), normalized mean absolute error (NME), and model rank, 2007–2009 November–May mean; $\mathrm{MAE} = \frac{1}{N}\sum_{i=1}^{N} |\mathrm{RF}_{\mathrm{Model}} - \mathrm{RF}_{\mathrm{Obs.}}|$; $\mathrm{NME} = \sum_{i=1}^{N} |\mathrm{RF}_{\mathrm{Model}} - \mathrm{RF}_{\mathrm{Obs.}}| (\sum_{i=1}^{N} \mathrm{RF}_{\mathrm{Obs.}})^{-1}$.

BGD
11, 17339–17360, 2014